JOURNAL OF AIRCRAFT
Vol. 33, No. 2, March–April 1996

# Prediction Method for Broadband Shock-Associated Noise from Supersonic Rectangular Jets

Christopher K. W. Tam*
*Florida State University, Tallahassee, Florida 32306-3027*
and
N. N. Reddy†
*Lockheed Martin Aeronautical Systems Company, Marietta, Georgia 30062-0685*

**A prediction method for broadband shock-associated noise from supersonic rectangular jets is developed. The noise prediction formula is designed primarily for jets issued from nozzles with straight sidewalls and with aspect ratio not more than six at the nozzle exit plane. For this type of supersonic rectangular jets two shock cell systems generally exist in the jet plume. One system starts at the nozzle exit plane as in the case of circular jets. The second system starts near the nozzle throat. The latter shock cell system does not vanish even when the jet is operating at its nominal design Mach number. Thus, there is broadband shock noise at all supersonic jet Mach numbers. The broadband shock noise prediction formula has been extended to include the effects of flight following the methodology used for circular jets.**

## I. Introduction

BROADBAND shock-associated noise is an important aircraft noise component of the proposed high-speed civil transport (HSCT) at takeoffs and landings. For noise certification purpose one would, therefore, like to be able to predict as accurately as possible the intensity, directivity, and spectral content of this noise component.

Recently, fairly accurate broadband shock-associated noise prediction formulas for circular supersonic jets have been developed.[1,2] These formulas are applicable to underexpanded as well as overexpanded jets. The effects of jet temperature and forward flight are also accounted for.[3,4] These prediction formulas are now a part of the NASA Aircraft Noise Prediction Program (ANOPP) shock noise prediction program. For rectangular supersonic jets, similar broadband shock-associated noise prediction methods do not exist at the present time. This is so, in spite of the fact that currently there are military jet aircrafts flying with rectangular nozzles in their propulsion systems.

The purpose of this work is to develop a semiempirical prediction method for the broadband shock-associated noise from supersonic rectangular jets. The complexity and quality of the noise prediction method are to be similar to those for circular jets. There are distinct differences in the flow and shock cell structures between supersonic rectangular and axisymmetric jets. As a result, there are significant differences between the shock noise emitted by these jets.[5]

In this article, only the broadband shock-associated noise of jets issued from rectangular nozzles with straight sidewalls is considered. Also, the nozzle aspect ratio is restricted to less than 6. In developing the prediction method the essential physics of the problem are taken into consideration. Since the broadband shock-associated noise generation mechanism is the same whether the jet is circular or rectangular, the present prediction method is quite similar to that for axisymmetric jets. Comparisons between predictions and measurements for jets with aspect ratio up to 6 will be reported. Efforts will be concentrated on the flyover plane. However, sideline angles and other directions will also be included.

The first part of this article concentrates on the case of jets in a static environment. The formulas developed are then extended to jets in flight following the formulation and methodology of Refs. 3 and 4. At the present time, however, noise data from rectangular jets in flight is not available in the literature. Thus, the flight noise prediction formula has yet to be tested.

## II. Basic Model and Methodology

Broadband shock-associated noise is generated by the weak interaction between the downstream propagating instability waves/large turbulence structures of the supersonic jet and the quasiperiodic shock cells in the jet plume. A comprehensive prediction theory of this noise generation process for circular imperfectly expanded jets was developed by Tam.[1–3] In developing the theory a stochastic model of the instability waves was used to represent the large turbulence structures. The spectra computed by the theory compared very favorably with the extensive measurements of Norum and Seiner,[6] Tanna et al.,[7] and Yamamoto et al.,[8] and the simulated flight data of Norum and Shearin.[9]

As in circular jets, broadband shock-associated noise is generated by the weak interaction between the downstream propagating instability waves/large turbulence structures and the quasiperiodic shock cells in rectangular supersonic jets. In rectangular jets the strength and characteristics of the shock cells and the instability waves/large turbulence structures are, however, quite different from those of circular jets. In deriving the new noise prediction formula the corresponding formula for circular jets is used as a starting point. The noise prediction formula for the flyover plane is developed first. An empirical correction factor is introduced for predictions in the sideline directions.

### A. Shock Cell Systems and Strengths

As pointed out by Tam et al.,[10] the shock cell structure of a jet is formed by the repeated reflections of the shocks/expansion fans generated at the nozzle lip off the mixing layer sur-

Presented as Paper 93-4387 at the AIAA 15th Aeroacoustics Conference, Long Beach, CA, Oct. 25–27, 1993; received July 28, 1994; revision received Sept. 8, 1995; accepted for publication Sept. 9, 1995. 

*Professor, Department of Mathematics; Consultant to Lockheed Martin Corporation, Marietta, GA. Associate Fellow AIAA.
†Head, Aeroacoustics Group. Senior Member AIAA.

rounding the jet. These shocks/expansion fans are generated by the mismatch of the static pressure inside and outside the jet. For underexpanded jets, the initial disturbance at the nozzle lip consists of expansion fans, whereas for overexpanded jets they are in the form of oblique shocks. In this work, only rectangular nozzles that are convergent–divergent in the minor axis (flyover) plane are considered. The sidewalls are straight without cutback. For this type of nozzle, a shock cell structure is formed by the trapping of disturbances initiated at the nozzle lip by the mixing layers on the four sides of the jet. However, because of the straight sidewalls a second shock cell system is formed, beginning at the nozzle throat. Both shock cell systems are responsible for broadband shock noise generation. If $M_j$ is the fully expanded jet Mach number, $M_d$ is the nozzle design Mach number and $\gamma$ is the ratio of the specific heats of the gas, then the strengths of the two shock cell systems are characterized by the parameters $(M_j^2 - M_d^2)/[1 + (\gamma - 1)/2M_d^2]$ and $(M_j^2 - 1)/[1 + (\gamma - 1)/2]$, respectively. (Since the second shock cell system starts at the nozzle throat the nozzle design Mach number has been set equal to unity.) For a rectangular jet with aspect ratio $\Lambda = b/h$ ($\Lambda > 1$), where $b$ and $h$ are the width and height of the nozzle at the jet exit, it is found empirically that the relative strength of the two shock cell systems depend on $\Lambda^2$. On accounting for the shock amplitude saturation effect due to nonlinearity,[2] the use of the following empirical formula for the square of the combined shock cell amplitude $\bar{A}^2$ has been found to give satisfactory broadband shock noise prediction:

$$\bar{A}^2 = \frac{\left\{\dfrac{M_j^2 - M_d^2}{1 + [(\gamma - 1)/2]M_d^2}\right\}^2 \dfrac{\Lambda^2}{1 + \Lambda^2}}{1 + \left(\left\{\dfrac{M_j^2 - M_d^2}{1 + [(\gamma - 1)/2]M_d^2}\right\}^2 \dfrac{\Lambda^2}{1 + \Lambda^2}\right)^{3/2}} + \frac{\left\{\dfrac{M_j^2 - 1}{1 + [(\gamma - 1)/2]}\right\}^2 \dfrac{1}{1 + \Lambda^2}}{1 + \left(\left\{\dfrac{M_j^2 - 1}{1 + [(\gamma - 1)/2]}\right\}^2 \dfrac{1}{1 + \Lambda^2}\right)^{3/2}} \tag{1}$$

### B. Shock Cell Modes and Spacings

In a rectangular jet the distance between mixing layers on the opposite sides of the jet in the major and minor axis plane can be quite different. Since the shock cell system is formed by the repeated reflections of the shocks/expansion fans off the mixing layers, the resulting structure is highly complex. Earlier, Tam[11] had developed a vortex sheet shock cell model for these jets. According to this model the pressure field associated with the shock cells is given by

$$p(x, y, z) = \sum_{n=1}^{\infty} \sum_{m=1}^{\infty} \frac{4\Delta p}{mn\pi^2} \cdot (1 - \cos n\pi)(1 - \cos m\pi) \times \sin\left(\frac{n\pi y}{b_j}\right) \sin\left(\frac{m\pi z}{h_j}\right) \cos(k_{mn}x) \tag{2}$$

$$k_{mn} = \left(\frac{n^2}{b_j^2} + \frac{m^2}{h_j^2}\right)^{1/2} \frac{\pi}{(M_j^2 - 1)^{1/2}}, \qquad m, n = 1, 2, \ldots \tag{3}$$

where $x$ is in the direction of the jet flow and the origin of the coordinate system is located at the lower left corner of the nozzle lip. The fully expanded width and height of the jet are $b_j$ and $h_j$, respectively. The two summations in Eq. (2) merely account for the reflections off the top and bottom and the left and right pairs of mixing layers surrounding the jet. In Eq. (3) $k_{mn}$ is the axial wave number of the $(m, n)$th shock cell mode. The corresponding shock cell spacing is given by $2\pi/k_{mn}$. Since the mixing layer of the jet is not infinitesimally thin, an empirical correction factor $c_m$ (independent of $n$) is introduced. For estimating the shock cell spacing of the $(m, n)$th mode, $k_{mn}c_m$ is to be used. These correction factors are

$$c_1 = \alpha_1 + [0.756 - 0.195M_j - (\alpha_1 - 1)]e^{-0.4(\Lambda-1)^2} \tag{4}$$

$$c_m = \alpha_1 + (1.1 - \alpha_1)e^{-0.4(\Lambda-1)^2}, \qquad m \geq 2 \tag{5}$$

where $\alpha_1 = 1.0 + 0.578e^{-4.75(M_j-1)^2}$.

### C. Convection Velocity of the Large Turbulence Structures/Instability Waves

For circular jets the convection velocity of the large turbulence structures/instability waves $u_c$ has been found experimentally by Harper-Bourne and Fisher[12] to be equal to 0.7 times the fully expanded jet velocity $u_j$. However, for rectangular jets the mean flow profile is different and it is not clear what the value of $u_c$ should be. If the aspect ratio of the jet is equal to one then the square jet would quickly become circular and the formula $u_c = 0.7u_j$ should be valid. On the other hand, when the aspect ratio of the jet is large the mean flow is basically two dimensional. In this case screech tone data indicate that $u_c/u_j$ is less than 0.7. Figure 1 shows the dependence of the screech tone frequencies of large aspect ratio cold rectangular jets on the jet Mach number measured by Powell,[13] Hammit,[14] and Krothapalli et al.[15] The full curve shows the predicted frequency as a function of jet Mach number calculated by Tam[11] using $u_c/u_j = 0.7$. The dotted curve shows the same calculation except that $u_c/u_j$ is taken to be 0.55. Clearly, a lower convection speed gives a better agreement with measurements. For the purpose of predicting broadband shock-associated noise from supersonic rectangular jets, it is believed that an empirical formula for $u_c/u_j$ compatible with the previous finding would provide better results than $u_c/u_j = 0.7$. After extensive testing it has been found that the following formula yields good predictions:

$$u_c/u_j = 0.5 + 0.2e^{-0.5(\Lambda-1)} \tag{6}$$

### D. Extension to Sideline Directions

In this work the noise prediction formula in the flyover plane was developed first. The prediction formula was then extended to the sideline directions by the subtraction of a sideline correction factor in decibels. The correction factor makes only a slight change in the decibel level. Its magnitude depends primarily on the nozzle aspect ratio $\Lambda$ and the azimuthal angle $\phi$

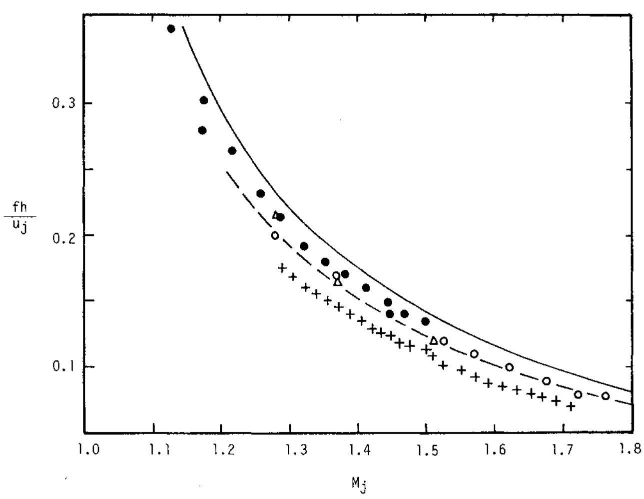


**Fig. 1 Comparison between measured and calculated screech tone frequencies of rectangular supersonic jets. ○, 3-mm nozzle; △, 5-mm nozzle, Ref. 15; ●, Ref. 13; +, Ref. 14; ——, $u_c/u_j = 0.7$; and – – –, $u_c/u_j = 0.55$.**

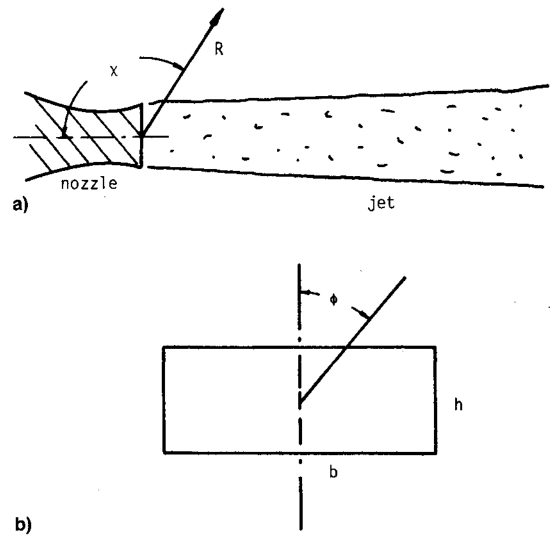


**Fig. 2 Schematic diagram showing the inlet angle $\chi$ and the azimuthal angle $\phi$ of the spherical coordinate system ($R$, $\chi$, $\phi$): a) side and b) end views.**

(see Fig. 2). The correction factor was developed entirely empirically based on the data of Ponton et al.[16] In decibel units the proposed correction factor $\Delta(\phi, \Lambda)$ is

$$\Delta(\phi, \Lambda) = (0.3992 - 0.5228\Lambda + 0.1192\Lambda^2)[\phi/(\pi/2)] + (-1.48 + 1.6764\Lambda - 0.192\Lambda^2)[\phi/(\pi/2)]^2 \quad (7)$$

where $\phi$ is in radians and is less than or equal to $\pi/2$.

## III. Broadband Shock-Associated Noise Prediction Formula

The input variables for the rectangular jet broadband shock-associated noise prediction formula are as follows:

$b$ = width of nozzle at the nozzle exit plane
$h$ = height of nozzle at the nozzle exit plane
$M_d$ = nozzle design Mach number
$M_j$ = fully expanded jet Mach number
$T_j$ = fully expanded jet temperature
$T_a$ = ambient gas temperature
$\rho_\infty$ = ambient gas density
$a_\infty$ = ambient sound speed
$\chi$ = inlet angle
$\phi$ = azimuthal angle measured from the flyover plane ($\leq \pi/2$)
$R$ = distance to observer
$\gamma$ = ratio of specific heats

With this input the aspect ratio of the jet $\Lambda = b/h$ and the jet velocity $u_j$ can be found immediately. In addition, the following physical quantities may also be calculated.

### A. Fully Expanded Jet Area and Dimensions

$$A_j = bh \frac{M_d}{M_j} \left\{ \frac{1 + [(\gamma - 1)/2]M_j^2}{1 + [(\gamma - 1)/2]M_d^2} \right\}^{(\gamma+1)/[2(\gamma-1)]}$$

$$h_j = A_j/b$$

$$b_j = b, \quad \text{nozzle with straight sidewalls}$$

### B. Odd and Even Mode Shock Cell Spacings

$$L_{mn} = \frac{2(M_j^2 - 1)^{1/2}}{\{[(2n-1)/b_j]^2 + [(2m-1)/h_j]^2\}^{1/2} c_m}$$

$$m, n = 1, 2, \ldots, 30$$

$$\hat{L}_m = \frac{2(M_j^2 - 1)^{1/2}}{[(1/b_j)^2 + (2m/h_j)^2]^{1/2} c_m}, \qquad m = 1, 2, \ldots, 3$$

where $c_m$ is the correction factor given by Eqs. (4) and (5).

### C. Half-Width of the Similarity Spectrum

$$x_c = \begin{cases} 4.3 + 1.2M_j^2, & T_j > T_a \\ 4.3 + 1.2M_j^2 + 1.2(1 - T_j/T_a), & T_j < T_a \end{cases}$$

$$L = 3x_c/8$$

### D. Peak Frequencies

$$f_{mn} = \frac{u_c}{L_{mn}(1 + M_c \cos\chi)}, \qquad m, n = 1, 2, 3, \ldots, 30$$

$$\hat{f}_m = \frac{u_c}{\hat{L}_m(1 + M_c \cos\chi)}, \qquad m = 1, 2, 3$$

where $M_c = u_c/a_\infty$ and $u_c$ is given by Eq. (6).

The proposed semiempirical noise spectral density formula for an observer with coordinates ($R$, $\chi$) in the flyover plane ($\phi = 0$) is

$$S(R, \chi, 0, f) = \frac{\bar{c}A_j\rho_\infty^2 a_\infty^4 M_j^2 \bar{A}^2}{R^2 f\{1 + [(\gamma-1)/2]M_j^2\}} \times \left( \sum_{m=1}^{30}\sum_{n=1}^{30} \frac{1}{(2m-1)^2(2n-1)[1 + 2(n-1)e^{-(\Lambda-1)}]} \times \exp\{-[(f_{mn}/f) - 1]^2(1 + M_c\cos\chi)^2 L^2(u_j/u_c)^2 \times [1/(2\,\ell n\,2)]\} + \sum_{m=1}^{3} \frac{1}{4m^2} \exp\{-[(\hat{f}_m/f) - 1]^2 \times (1 + M_c\cos\chi)^2 L^2(u_j/u_c)^2[1/(2\,\ell n\,2)]\} \right) \times \begin{pmatrix} A_j/bh, & \text{overexpanded jet} \\ 1, & \text{underexpanded jet} \end{pmatrix} \quad (8)$$

where $f$ is the frequency, $\bar{c} = 2.886 \times 10^{-4}$, and $\bar{A}^2$ is given by Eq. (1).

Finally, for an observer with polar coordinates ($R$, $\chi$, and $\phi$), not necessarily on the flyover plane, the formula for the noise spectral density in decibels is

$$S(R, \chi, \phi, f) = S(R, \chi, 0, f) \text{ in dB} - \Delta(\phi, \Lambda) \text{ in dB} \quad (9)$$

where $\Delta(\phi, \Lambda)$ is given by Eq. (7).

## IV. Comparisons with Experiments

A set of high-quality broadband shock noise data from supersonic rectangular jets is provided in the work of Ponton et al.[16] In their experiments three rectangular nozzles with aspect ratio less than 6 were used. The far-field narrow-band spectrum measurements at 60-Hz bandwidth covered a large range of inlet and azimuthal angles. The jet Mach numbers varied from overexpanded to highly underexpanded operating conditions.

Figure 3 shows a comparison between the measured and the calculated shock noise spectrum [Eq. (8)] at 60-Hz bandwidth for a rectangular jet of aspect ratio 5.325, nozzle design Mach

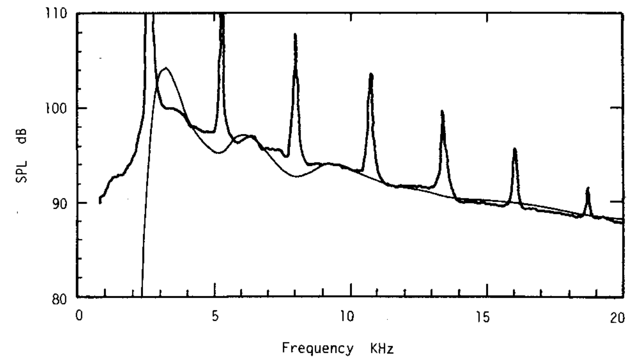


**Fig. 3 Comparison between calculated and measured shock noise spectrum. Aspect ratio = 5.325, $M_j$ = 1.608, $M_d$ = 1.35, $\chi$ = 45 deg, and $\phi$ = 0 deg.**

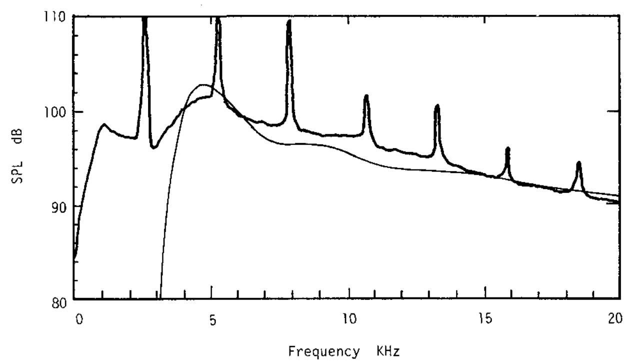


**Fig. 4 Comparison between calculated and measured shock noise spectrum. Aspect ratio = 5.325, $M_j$ = 1.608, $M_d$ = 1.35, $\chi$ = 90 deg, and $\phi$ = 0 deg.**

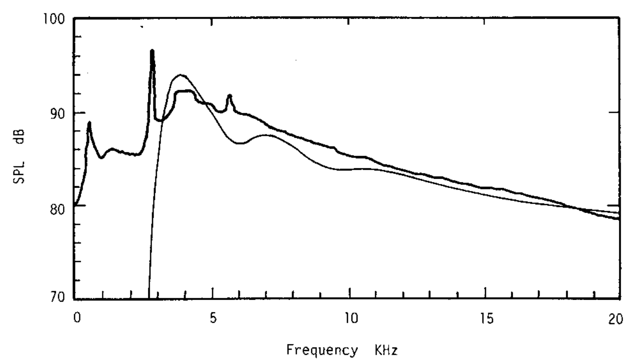


**Fig. 5 Comparison between calculated and measured shock noise spectrum. Aspect ratio = 3.398, $M_j$ = 1.35, $M_d$ = 1.35, $\chi$ = 45 deg, and $\phi$ = 0 deg.**

number 1.35, and fully expanded jet Mach number of 1.608. The microphone was located at $\chi$ = 45 deg and $\phi$ = 0 deg. Notice that for a large aspect ratio jet the spectrum is dominated by a screech tone and its harmonics. As can be seen, the predicted spectrum matches well with the measurement. Figure 4 shows the spectrum at $\chi$ = 90 deg in the flyover plane. There is again good agreement between the predicted and the measured spectrum.

Figures 5 and 6 provide comparisons between the calculated and the measured noise spectra of an aspect ratio 3.398 nozzle at an operating Mach number of 1.35. This Mach number is also equal to the nominal design Mach number of the nozzle. However, because the sidewalls of the nozzle are straight there is still a shock cell structure in the jet plume. As a result there is still a significant amount of broadband shock noise. Figure 5 is for $\chi$ = 45 deg in the flyover plane. Figure 6 is for $\chi$ = 90 deg. It is seen that the predicted spectra agree well with the measurements.

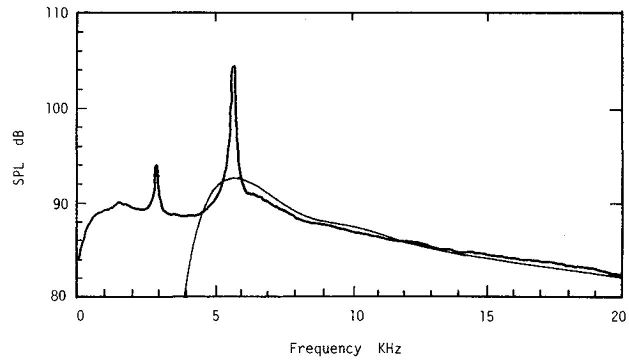


**Fig. 6 Comparison between calculated and measured shock noise spectrum. Aspect ratio = 3.398, $M_j$ = 1.35, $M_d$ = 1.35, $\chi$ = 90 deg, and $\phi$ = 0 deg.**

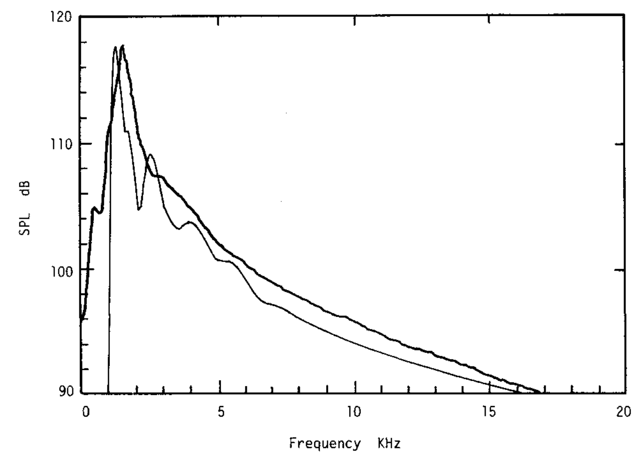


**Fig. 7 Comparison between calculated and measured shock noise spectrum. Aspect ratio = 1.538, $M_j$ = 1.904, $M_d$ = 1.66, $\chi$ = 45 deg, and $\phi$ = 0 deg.**

As the aspect ratio of the jet is reduced and approaches unity, the noise of the jet becomes more axisymmetric and resembles that of a circular jet. Figures 7 and 8 show the noise spectrum of an aspect ratio 1.538 jet at a jet Mach number of 1.904. The nozzle design Mach number is 1.66. The shock noise spectra are dominated by a single peak with rapid drop-off as frequency increases. The spectral shape is quite different from those of the large aspect ratio jets shown in Figs. 3 and 4. The spectra given in Fig. 7 are at an inlet angle of 45 deg in the flyover plane whereas those given in Fig. 8 are at an inlet angle of 90 deg. The calculated spectra again match quite well with the measurements.

Figures 9–11 provide comparisons between the calculated and the measured noise spectra at $\phi$ = 90 deg (or on the major axis plane of the nozzle) at $\chi$ = 45 deg. The data in Fig. 9 are from the aspect ratio 5.325 nozzle jet at a jet Mach number of 1.507. Figure 10 shows the spectra of the aspect ratio 3.398 nozzle jet at an overexpanded jet Mach number of 1.23. Figure 11 is for the aspect ratio 1.538 nozzle jet at $M_j$ = 1.807. As can readily be seen the agreements between the predictions and measurements are reasonably good in all cases.

Extensive comparisons between measurements and Eq. (8) beyond those discussed earlier have been carried out. Overall favorable agreements are found. The agreements are, however, better in the flyover plane.

## V. Flight Effects

For community noise prediction applications it is necessary to extend Eq. (8) to include the effects of flight. Here this is carried out following the methodology developed in Ref. 4 for circular jets.

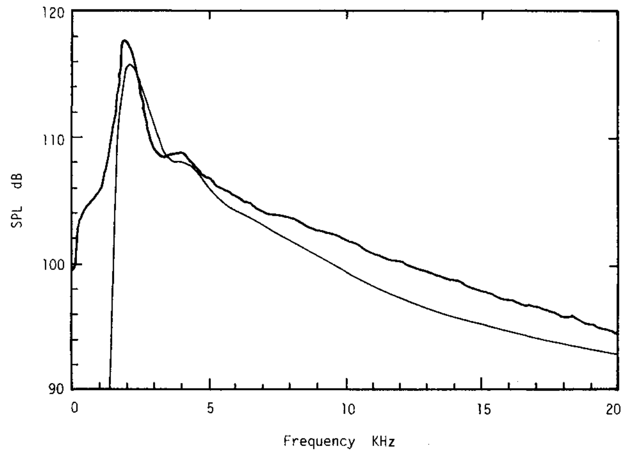


**Fig. 8 Comparison between calculated and measured shock noise spectrum. Aspect ratio = 1.538, $M_j$ = 1.904, $M_d$ = 1.66, $\chi$ = 90 deg, and $\phi$ = 0 deg.**

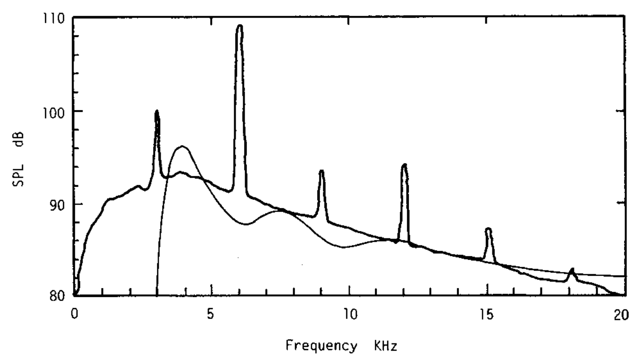


**Fig. 9 Comparison between calculated and measured shock noise spectrum. Aspect ratio = 5.325, $M_j$ = 1.507, $M_d$ = 1.35, $\chi$ = 45 deg, and $\phi$ = 90 deg.**

Consider a jet flying horizontally at a velocity $u_f$ and flight Mach number $M_f$ ($M_f < 1$) as shown in Fig. 12. Let $\chi_e$ and $R_e$ be the emission angle and distance, respectively. This is the angle and distance to the observer when the sound waves are generated by the jet at location $A$. By the time the sound waves reach the ground observer the jet would have moved to $B$. The angle $\chi$ and distance $R$ are the coordinates of the observer at reception time. Clearly, the distance $AB$ is equal to $M_f R_e$. By the cosine and sine laws of the triangles $OAB$ it is easy to find:

$$R = R_e(1 + M_j^2 - 2M_f \cos \chi_e)^{1/2} \tag{10}$$

$$\chi = \begin{cases} \sin^{-1}\left[\dfrac{\sin \chi_e}{(1 + M_j^2 - 2M_f \cos \chi_e)^{1/2}}\right], & \text{if} \quad \cos \chi_e > M_f \\ \pi - \sin^{-1}\left[\dfrac{\sin \chi_e}{(1 + M_f^2 - 2M_f \cos \chi_e)^{1/2}}\right], & \text{otherwise} \end{cases} \tag{11}$$

In Ref. 4 the flight effects were formulated in the reception coordinates. This will be followed here. In constructing noise footprints or other similar applications it is sometimes more convenient to specify the emission coordinates. When such a situation arises it is, however, a simple matter to convert them to the reception coordinates by Eqs. (10) and (11).

Flight effects on broadband shock noise can, broadly speaking, be divided into two types as pointed out in Ref. 3. The first type involves noise source modifications. This includes, for instance, the stretching of the shock cells, the increase in convection velocity of the large turbulence structures/instability waves relative to the nozzle, and changes in the characteristics of the turbulence/instability wave spectrum. The second type involves kinematic effects such as Doppler frequency shift and sideline intensity enhancement. For detailed analysis of these effects the readers are referred to Ref. 3.

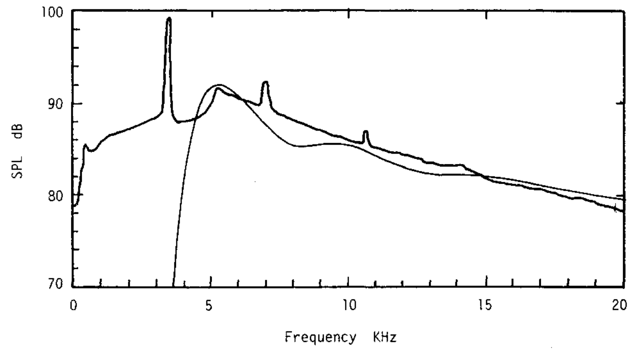


**Fig. 10 Comparison between calculated and measured shock noise spectrum. Aspect ratio = 3.389, $M_j$ = 1.23, $M_d$ = 1.35, $\chi$ = 45 deg, and $\phi$ = 90 deg.**

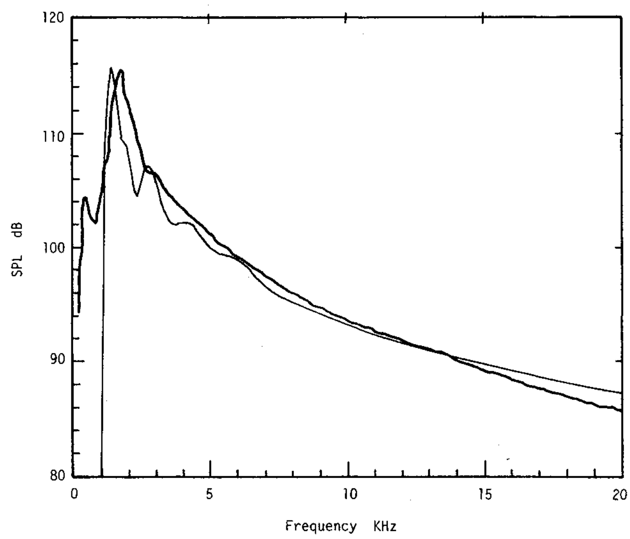


**Fig. 11 Comparison between calculated and measured shock noise spectrum. Aspect ratio = 1.538, $M_j$ = 1.807, $M_d$ = 1.66, $\chi$ = 45 deg, and $\phi$ = 90 deg.**

On following the analysis and proposed modifications of Ref. 4 the formulas for the turbulence convection velocity, half-width of the similarity spectrum, and shock cell spacings for jets in flight are

Convection velocity:

$$\frac{u_c}{u_j} = \left[0.5 + 0.2e^{-0.5(\Lambda-1)} - 0.06\left(\frac{T_t}{T_a} - 1.0\right)\right] \times \left(1 - \frac{u_f}{u_j}\right) + \frac{u_f}{u_j} \tag{12}$$

where $T_t$ is the total temperature of the jet.

Half-width of the similarity spectrum:

$$x_c = \begin{cases} 4.3 + 1.2M_j^2 & T_j > T_a \\ 4.3 + 1.2M_j^2 + 1.2(1 - T_j/T_a) & T_j < T_a \end{cases} \tag{13}$$

$$L = 3.0(x_c/8.0)\{1.0 + [1.114 - 0.36(T_j/T_a)]M_f\} \tag{14}$$

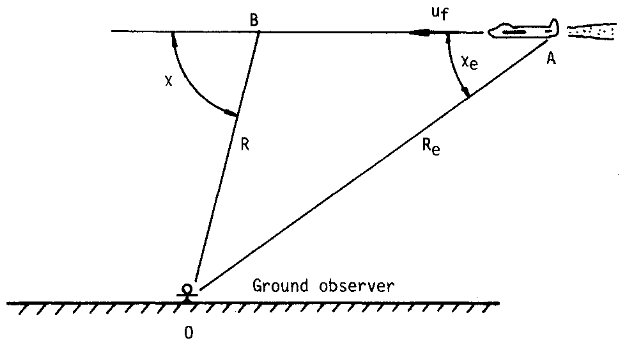


**Fig. 12 Schematic diagram showing the geometrical relation between emission angle and distance and reception angle and distance for a jet in level flight.**

Shock cell spacings:

$$L_{mn} = \frac{2(M_j^2 - 1)^{1/2}[1.0 + (0.812 - 0.254T_j/T_a)M_f]}{\{[(2n - 1)/b_j]^2 + [(2m - 1)/h_j]^2\}^{1/2} c_m}$$

$$m = 1, 2, 3, \ldots, 30, \qquad n = 1, 2, 3, \ldots, 30$$

$$\hat{L}_m = \frac{2(M_j^2 - 1)^{1/2}[1.0 + (0.812 - 0.254T_j/T_a)M_f]}{[(1/b_j)^2 + (2m/h_j)^2]^{1/2} c_{2m}}$$

$$m = 1, 2, 3$$

where $c_m$ is as before the correction factor given by Eqs. (4) and (5).

The noise spectral density in the flyover plane is

$$S(R, \chi, 0, f) = \frac{\bar{c}A_j \rho_\infty^2 a_\infty^4 M_j^2 \bar{A}^2}{R^2 f(1 - M_f^2 \sin^2\chi)\left(1 + \frac{\gamma - 1}{2} M_j^2\right)}$$

$$\times \left\{ \sum_{m=1}^{30} \sum_{n=1}^{30} \frac{e^{-\left[\frac{u_c}{L_{mn}(z - M_f \cos\chi)zf} - 1 - \frac{M_c(\cos\chi + M_f z)}{z(1 - M_f^2)}\right]^2 \left(\frac{u_j}{u_c}\right)^2 \frac{L^2}{2\ell n 2}}}{(2m - 1)^2(2n - 1)[1 + 2(n - 1)e^{-(\Lambda - 1)}]} \right.$$

$$\left. + \sum_{m=1}^{3} \frac{e^{-\left[\frac{u_c}{\hat{L}_m(z - M_f \cos\chi)zf} - 1 - \frac{M_c(\cos\chi + M_f z)}{z(1 - M_f^2)}\right]^2 \left(\frac{u_j}{u_c}\right)^2 \frac{L^2}{2\ell n 2}}}{4m^2} \right\}$$

$$\times \begin{pmatrix} A_j/bh, & \text{overexpanded jets} \\ 1, & \text{underexpanded jets} \end{pmatrix} \qquad (15)$$

where $z = (1 - M_f^2 \sin^2\chi)^{1/2}$. For observers not in the flyover plane Eq. (9) still applies provided that $S(R, \chi, 0, f)$ is calculated by Eq. (15).

## VI. Summary

A semiempirical broadband shock-associated noise prediction formula for rectangular supersonic jets issuing into a static external environment has been developed. The formula is designed for rectangular nozzles with straight sidewalls and aspect ratio less than 6. Extensive comparisons between the measured data of Ponton et al.[16] and the calculated noise spectra have been carried out. Favorable agreement is observed.

Extension of the noise prediction formula to jets in flight has been carried out. Because of the lack of measured data the extended formula has yet to be validated.

## Acknowledgments

This work was supported by the Aeroacoustics Branch of NASA Langley Research Center through Lockheed Martin Engineering and Sciences Company of Hampton, Virginia (work order 087-OR-028). The authors wish to thank Robert A. Golub of NASA Langley Research Center for his technical support.

## References

[1]Tam, C. K. W., "Stochastic Model Theory of Broadband Shock Associated Noise from Supersonic Jets," *Journal of Sound and Vibration*, Vol. 116, No. 2, 1987, pp. 265–302.

[2]Tam, C. K. W., "Broadband Shock Associated Noise of Moderately Imperfectly Expanded Supersonic Jets," *Journal of Sound and Vibration*, Vol. 140, No. 1, 1990, pp. 55–71.

[3]Tam, C. K. W., "Broadband Shock Associated Noise from Supersonic Jets in Flight," *Journal of Sound and Vibration*, Vol. 151, No. 1, 1991, pp. 131–147.

[4]Tam, C. K. W., "Broadband Shock Associated Noise from Supersonic Jets Measured by a Ground Observer," *AIAA Journal*, Vol. 30, No. 10, 1992, pp. 2395–2401.

[5]Seiner, J. M., Ponton, M. K., and Manning, J. C., "Acoustic Properties Associated with Rectangular Geometry Supersonic Nozzles," AIAA Paper 86-1867, July 1986.

[6]Norum, T. D., and Seiner, J. M., "Measurements of Mean Static Pressure and Far Field Acoustics of Shock-Containing Supersonic Jets," NASA TM 84521, Sept. 1983.

[7]Tanna, H. K., Dean, P. D., and Burrin, R. H., "The Generation and Radiation of Supersonic Jet Noise. Volume IV, Shock Associated Noise Data," Air Force Aero-Propulsion Lab., AFAPL-TR-76-65, Wright–Patterson AFB, OH, Sept. 1976.

[8]Yamamoto, K., Brausch, J. F., Janardan, B. A., Hoerst, D. J., Price, A. O., and Knott, P. R., "Experimental Investigation of Shock-Cell Noise Reduction for Single-Stream Nozzles in Simulated Flight, Comprehensive Data Report, Volume 1," NASA CR-168234, May 1984.

[9]Norum, T. D., and Shearin, J. G., "Shock Structure and Noise of Supersonic Jets in Simulated Flight to Mach 0.4," NASA TP 3785, Feb. 1988.

[10]Tam, C. K. W., Jackson, J. A., and Seiner, J. M., "A Multiple-Scale Model of the Shock-Cell Structure of Imperfectly Expanded Supersonic Jets," *Journal of Fluid Mechanics*, Vol. 153, April 1985, pp. 123–149.

[11]Tam, C. K. W., "The Shock-Cell Structures and Screech Tone Frequencies of Rectangular and Non-Axisymmetric Supersonic Jets," *Journal of Sound and Vibration*, Vol. 121, No. 1, 1988, pp. 135–147.

[12]Harper-Bourne, M., and Fisher, M. J., "The Noise from Shock Waves in Supersonic Jets," *Proceedings of the AGARD 131st Conference on Noise Mechanisms*, AGARD, Brussels, Belgium, 1974, pp. 11-1–11-13.

[13]Powell, A., "On the Noise Emanating from a Two Dimensional Jet Above the Critical Pressure," *Aeronautical Quarterly*, Vol. 4, Pt. 2, Feb. 1953, pp. 103–122.

[14]Hammitt, A. G., "The Oscillation and Noise of an Overpressure Sonic Jet," *Journal of Aerospace Sciences*, Vol. 28, Sept. 1961, pp. 673–680.

[15]Krothapalli, A., Hsia, Y., Baganoff, D., and Karamcheti, K., "The Role of Screech Tones on Mixing of an Underexpanded Rectangular Jet," *Journal of Sound and Vibration*, Vol. 106, No. 1, 1986, pp. 119–143.

[16]Ponton, M. K., Manning, J. C., and Seiner, J. M., "Far-Field Acoustics of Supersonic Rectangular Nozzles with Various Throat Aspect Ratios," NASA TM 89002, Dec. 1986.